BCS-like T_c does not necessarily imply BCS pairing mechanism: The case of magnetically mediated quantum critical pairing

Yuxuan Wang[1] and Andrey V. Chubukov[2]

[1]*Department of Physics, University of Florida, Gainesville, Florida 32601, USA*
[2]*School of Physics and Astronomy and William I. Fine Theoretical Physics Institute, University of Minnesota, Minneapolis, Minnesota 55455, USA*

In the BCS theory of superconductivity, an instability towards pairing develops at arbitrarily weak dimensionless coupling λ due to a divergence of logarithmic perturbative series for the pairing susceptibility (Cooper logarithms) at $T_c \sim \omega_0 e^{-1/\lambda}$, where ω_0 is an energy cutoff. On the contrary, in many models of superconductivity out of a non-Fermi-liquid, the Cooper logarithm is absent, and superconductivity emerges only when λ exceeds a certain threshold. We argue that there are situations when there is no threshold, and at weak coupling the formula for T_c is BCS-like, yet the origin of the pairing instability is fundamentally different from that in the BCS scenario. As an example, we revisit superconductivity in a metal at the onset of (π, π) spin-density-wave order. Earlier studies of this problem found no threshold and a BCS-like expression for T_c at weak coupling. We argue that, despite this, the pairing is not caused by the Cooper logarithm, and in many respects it is qualitatively similar to that in non-Fermi-liquids.

I. INTRODUCTION

Non-BCS pairing of fermions from a non-Fermi-liquid normal state has attracted substantial interest in recent years in both condensed-matter and high-energy communities. In a nutshell, pairing out of a non-Fermi-liquid is mediated by a massless boson, the same one that destroys Fermi-liquid behavior. This leads to a nontrivial competition between two opposite tendencies, one towards pairing and the other towards a non-Fermi-liquid. In some cases, this competition leads to superconductivity with enhanced critical temperature T_c [1–7], while in others it leads to a complete suppression of pairing such that the system remains metallic down to zero temperature [2,8,9]. In both cases, strong pairing fluctuations above T_c give rise to a pseudogap behavior [6,10].

In a Fermi liquid with a weak attractive interaction, pairing instability develops via the well-known BCS mechanism. Namely, the pairing susceptibility χ_{pp} is expressed within perturbation theory via a power series of a Cooper logarithm—the term $\lambda \log(\omega_0/T)$, where λ is a dimensionless coupling, ω_0 is an energy cutoff, and T is the temperature. The series is geometrical and yields $\chi_{pp} \propto 1/[1 - \lambda \log(\omega_0/T)]$, which diverges at $T = T_c \sim \omega_0 e^{-1/\lambda}$, signaling the onset of superconductivity.

By contrast, in non-Fermi-liquids, such as quantum-critical metals [2,3,6,8,11–13] and Yukawa-SYK models [9,14–23] of dispersionless fermions with random interactions, perturbation series for χ_{pp} are rather peculiar: they are logarithmic, as in BCS theory, but the argument of the logarithm depends on the running frequency of a fermion, ω, and the combinatorial factor for the nth term in the series is $1/n!$ rather than 1. The series $\lambda^n |\log(\omega_0/|\omega|)|^n / n!$ sum up into $\chi_{pp}(\omega) \propto (\omega_0/|\omega|)^\lambda$, which does not diverge at any finite

frequency, i.e., any finite T.[1] To search for a potential pairing instability, one has to go beyond the expansion in powers of the logarithms and compute the pairing susceptibility exactly. The outcome of the exact analysis is that the pairing instability develops, but only if λ exceeds a certain threshold λ_c, when nonlogarithmic corrections change the exponent for $\chi_{pp}(\omega)$ to the extent that it becomes complex and $\chi_{pp}(\omega)$ develops oscillations. Such behavior cannot be captured within order-by-order expansion and indicates a breakdown of perturbation theory in the particle-particle channel. Solving the nonlinear gap equation for the gap function $\Delta(\omega)$, one then finds that this breakdown implies an instability towards superconductivity. This is often referred to as the *complex exponent* scenario of the pairing rather than the one based on the summation of the Cooper logarithms.[2]

There is one additional aspect in which this pairing differs from BCS. Namely, the nonlinear gap equation has an infinite number of topologically distinct solutions, which differ in the number of oscillations of $\Delta_n(\omega)$. Each solution has its own $T_{c,n}$. The largest $T_{c,0}$ is for nonoscillating $\Delta_n(\omega)$, which is a global minimum of the condensation energy. Other solutions are saddle points. In BCS theory, there exists a single solution for a superconducting order parameter at $T < T_c$ (the same

---

[1]Within the renormalization-group (RG) framework, the coupling constant g in the Cooper channel flows to a fixed point instead of running to infinity.

[2]In the RG language, the fixed points for g formally move to the complex plane and become inaccessible [8,9,24,25], and instead g flows all the way to infinity. A similar scenario has been proposed to describe the pseudocritical behavior at putative deconfined quantum phase transitions [26,27].

holds in the Eliashberg theory for pairing out of a Fermi liquid [28]).

In a recent paper [29], Ojajarvi *et al.* analyzed unconventional superconductivity in a 2D system with Hubbard-like repulsion U, near a single van Hove point. They found that p-wave superconductivity develops already for an arbitrarily small U, and that $T_c \propto e^{-1/\lambda}$, where $\lambda \propto U$. On the surface, this looks like BCS pairing. The authors of Ref. [29], however, argued that there is no Cooper logarithm for this problem, and the exponential dependence of T_c on λ is due to logarithmic singularity in the density of states at the van Hove point. They argued that the pairing mechanism is very similar to the one for non-BCS pairing mediated by a massless boson. In particular, the pairing instability is a consequence of oscillations in $g(E)$, and there exists an infinite number of $T_{c,n}$ with a topologically distinct gap function, of which $T_{c,0}$ is the largest.

In this paper, we argue that the same holds for d-wave pairing in a metal near the onset of a spin-density-wave order with momentum (π, π). This pairing has been extensively analyzed in the context of cuprate and pnictide superconductors and other materials. At and above optimal doping, the cuprates display metallic behavior and the Fermi surface area matches the Luttinger count, and magnetic-mediated pairing is often thought to be confined to the area near hot spots—$\boldsymbol{k}_F$ points for which $\boldsymbol{k}_F + (\pi, \pi)$ is also on the Fermi surface. The fermionic self-energy $\Sigma(\omega)$ right at a hot spot is singular, scaling as $\omega^{1/2}$. Such pairing of hot fermions then falls into the "pairing out of non-Fermi-liquid" category, in which superconductivity only develops when the pairing interaction is above the threshold. However, for lukewarm fermions away from hot spots, the self-energy $\Sigma(\omega_m, k_\parallel) \propto \omega/|k_\parallel|$ [30], where $k_\parallel$ is the momentum deviation from a hot spot along the Fermi surface. Intuitively, as these fermions retain Fermi liquid behavior at any $k_\parallel$, they can pair at arbitrarily weak d-wave interaction λ and, by proximity, impose pairing of hot fermions. Indeed, explicit calculations show [3] that $T_c \propto e^{-1/\lambda}$, i.e., that it has the same functional form as in BCS theory. Although the result looks like BCS pairing of lukewarm fermions, we argue that this is not the case, and, despite the similarity with the BCS formula for T_c, the pairing mechanism is fundamentally non-BCS and is rather similar to the previous case for fermions near a single van Hove point.

To prove our point, we note that although a lukewarm fermion has a frequency dependence that is Fermi-liquid-like and linear in ω, the prefactor critically depends on the distance from a hot spot, so some non-Fermi-liquid physics can be expected. We analyze the linearized gap equation for the pairing vertex Φ, and we show that the pairing at weak coupling falls into the "complex exponent" scenario. In fact, a perturbative analysis of the pairing susceptibility yields a power series of $\log^2(\Lambda/T)$, but their sum does not diverge [3]. As a consequence of the complex exponents (oscillation of Φ), there is an infinite set of $T_{c,n}$. We first convert the original integral equation into a differential form, and we begin with an analysis of a simplified toy model, which can be straightforwardly solved. Then we analyze the full differential equation, find its exact solution, and show that the pairing mechanism remains the same as in the toy model.

Finally, we show that this differential equation can be directly mapped to the renormalization-group (RG) equation for the coupling constant in the Cooper channel. The RG formulation of our pairing problem makes it clear that the pairing mechanism is fundamentally different from the BCS mechanism.

The structure of the paper is the following. In Sec. II we provide some background information about the model and present the gap equation for pairing between lukewarm fermions, which will be the point of departure for our analysis. Here we also show that the BCS-type iteration procedure based on the summation of the leading powers of logarithms yields no pairing instability. In Sec. III we convert the integral gap equation into a differential one and analyze it. We start in Sec. III A with the simplified differential equation, with which we show that the pairing mechanism is the same as that for the pairing out of a non-Fermi-liquid, but T_c is nonzero for arbitrarily weak λ and has BCS-like form $T_c \propto e^{-c/\lambda}$, where $c = \pi/4$. In Secs. III B and III C we analyze the full differential equation, and we show that the mechanism of pairing remains the same as in the toy model, and T has the same form at the smallest ϵ. In Sec. III D we discuss a more accurate mapping of the integral equation into a differential one, which extends beyond previous conversions and also borrows some results from [3]. We argue that this gives an accurate result $T_c \propto e^{-1/\lambda}$ (i.e., $c = 1$). In Sec. IV we reformulate our pairing problem in the RG framework, which makes clear its fundamental difference with BCS. We show that the RG equation is fully equivalent to the differential equation for the pairing vertex [31]. We present our conclusions in Sec. V. For completeness, in Appendix A we follow Ref. [31] and analyze the interplay between the differential gap equation, extracted from the Eliashberg theory, and the RG equation for the flow of the running coupling for two intensively studied dynamical models: the one with a logarithmic (color superconductivity) and power-law (the γ-model) dynamical interaction. In Appendix B we compare this work with our 2013 paper on the same subject, Ref. [3].

II. BACKGROUND: MODEL AND INTEGRAL GAP EQUATION

We follow earlier works [2,30,32–35] and analyze the pairing near an antiferromagnetic QCP within the semiphenomenological spin-fermion model. The model assumes that antiferromagnetic correlations develop already at high energies, of order bandwidth, and mediate interactions between low-energy fermions. The static part of the spin-fluctuation propagator is treated as a phenomenological input from high-energy physics, but the dynamical Landau damping part is self-consistently obtained within the model as it comes entirely from low-energy fermions [2,30,34]. We assume, as in those earlier works, that the Eliashberg approximation (no corrections to the spin-fermion vertex and the self-consistent one-loop approximation for the self-energy) is valid in a wide range of frequencies, which extends below the ones relevant for the pairing. For a detailed analysis of the validity of the Eliashberg theory for a spin-fermion model, see, e.g., Refs. [30,34,36,37].
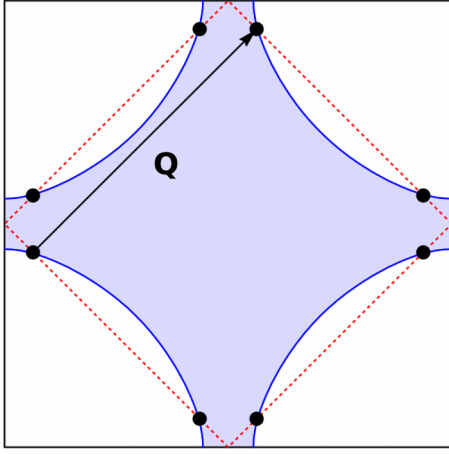
FIG. 1. The Fermi surface near a quantum-critical point of antiferromagnetic order. The hot spots are labeled as black dots, connected by the wave vector $\boldsymbol{Q}$ of the order parameter.

The action of the spin-fermion model is given by [30,34,38]

$$\mathcal{S} = -\int_k G_0^{-1}(k)\psi_{k,\alpha}^{\dagger}\psi_{k,\alpha} + \frac{1}{2}\int_q \chi_0^{-1}(q)\,\boldsymbol{S}_q \cdot \boldsymbol{S}_{-q}$$
$$+ \int_{k,q} \psi_{k+q,\alpha}^{\dagger}\boldsymbol{\sigma}_{\alpha\beta}\psi_{k,\beta} \cdot \boldsymbol{S}_{-q}, \quad (1)$$

where $\int_k$ stands for the integral over $\boldsymbol{k}$ and the sum over Matsubara frequencies, $G_0(k) = G_0(\omega_m, \boldsymbol{k}) = 1/[i\omega_m - \boldsymbol{v}_{F,\boldsymbol{k}} \cdot (\boldsymbol{k} - \boldsymbol{k}_F)]$ is the bare fermion propagator, $\chi_0(q) = \lambda/\boldsymbol{q}^2$ is the static propagator of collective bosons at quantum criticality, and $\boldsymbol{q}$ is measured with respect to $\boldsymbol{Q}$.

A. Hot and lukewarm fermions

Antiferromagnetic fluctuations are peaked at $\boldsymbol{Q} = (\pi, \pi)$, and mostly affect fermions located near hot spots—Fermi surface points $\boldsymbol{k}_F$, for which $\boldsymbol{k}_F + \boldsymbol{Q}$ is also at the FS; see Fig. 1. The Fermi velocities at hot spots separated by $\boldsymbol{Q}$ can be expressed as $\boldsymbol{v}_{F,1} = (v_x, v_y)$ and $\boldsymbol{v}_{F,2} = (-v_x, v_y)$, where the x axis is along $\boldsymbol{Q}$.

Without loss of generality, we set $v_x = v_y$ in this work.

The fermion-boson coupling gives rise to fermionic and bosonic self-energies. In the normal state, bosonic self-energy accounts for Landau damping of spin excitations, while fermionic self-energy accounts for mass renormalization and a finite lifetime of a fermion. At the one-loop level [30,34],

$$\Sigma(\omega_m, k_{\parallel}) = \frac{3\lambda}{4\pi v_F}\frac{2\omega_m}{\sqrt{\gamma|\omega_m| + k_{\parallel}^2} + |k_{\parallel}|}, \quad (2)$$

$$\chi(\Omega_m, \boldsymbol{q}) = \frac{\lambda}{\boldsymbol{q}^2 + |\Omega_m|\gamma}, \quad (3)$$

where $\omega_m = \pi T(2m + 1)$ is the fermionic Matsubara frequency, $\gamma = 4\lambda/(\pi v_F^2)$, and $k_{\parallel}$ is the deviation from a hot spot along the FS. The fermionic self-energy right at a hot spot has a non-FL form:

$$\Sigma(\omega_m, 0) = \sqrt{\omega_0|\omega_m|}\,\mathrm{sgn}(\omega_m), \quad (4)$$

where $\omega_0 = 9\lambda/16\pi$. For fermions away from the hot spot, known as the "lukewarm fermions," $\Sigma(\omega_m, k_{\parallel})$ retains a FL form at the smallest ω_m and scales as

$$\Sigma(\omega_m, k_{\parallel}) \approx \sqrt{\gamma\omega_0}\,\frac{\omega_m}{2|k_{\parallel}|}, \quad k_{\parallel}^2 \gg \gamma\omega_m. \quad (5)$$

B. Integral gap equation

These normal-state results are inputs for the analysis of the pairing. The linear gap equation for pairing between fermions near two hot spots has been obtained within the Eliashberg approximation in [3], and is

$$\Phi(k_{\parallel}, \omega_m) = \frac{\epsilon\lambda}{2v_F}T\sum_{m'}\int\frac{dk'_{\parallel}}{2\pi}\frac{1}{|\omega'_m + \Sigma(\omega'_m, k'_{\parallel})|}$$
$$\times \frac{\Phi(k'_{\parallel}, \omega'_m)}{k_{\parallel}^2 + k'^2_{\parallel} + \gamma|\omega_m - \omega'_m|}. \quad (6)$$

The parameter ϵ is the relative strength of the spin-mediated interactions in the d-wave particle-particle channel and the s-wave particle-hole channel. We follow Refs. [2,3,11,30] and treat ϵ as a small parameter.[3] For simplicity, below we will refer to (6) as the gap equation.

1. Pairing out of non-Fermi-liquid

In the pioneering study of the pairing in the spin-fermion model [2], Abanov *et al.* assumed that the pairing predominantly comes from hot fermions, for which the self-energy is given by (4). Upon substituting this self-energy into (6), setting $k_{\parallel} = 0$, and integrating over $k'_{\parallel}$, the gap equation takes the universal form[4]

$$\Phi(\omega_m) = \frac{\epsilon T}{4}\sum_{\omega_{m'}}\frac{\sqrt{\omega_0}}{|\omega_{m'} + \Sigma(\omega_{m'})|}\frac{\Phi(\omega_{m'})}{|\omega_m - \omega'_m|^{1/2}}. \quad (7)$$

The temperature at which this equation has a nonzero solution is the onset of pairing. In the absence of strong phase fluctuations, this is superconducting T_c.

The solution of the gap equation is the following [2,39,40]. First, there is a threshold for the pairing, i.e., T_c is finite only at $\epsilon > \epsilon_c = 0.22$. Near the threshold, $T_c \sim \omega_0 \exp[-b/(\epsilon - \epsilon_c)^{1/2}]$, $b \approx 3.41$ (for similar results in other systems, see [24,25]). Second, the pairing instability does not come from the summation of Cooper logarithms and is revealed only by going beyond the logarithmic approximation. Third, there is a tower of critical temperatures, $T_{c,n}$, which all emerge once ϵ exceeds ϵ_c and scale as $\omega_0 \exp[-b_n/(\epsilon - \epsilon_c)^{1/2}]$. The T_c given above is the largest $T_{c,0}$. Each $T_{c,n}$ signals an instability towards a state with topologically distinct $\Phi(\omega_m)$.

---

[3]This can be justified by, e.g., formally extending the model to a matrix large-N theory [8], in which case $\epsilon = 1/N$ [39,40].

[4]Equation (7) is a specific realization of the pairing in the γ-model—a generic model of pairing out of a non-Fermi-liquid by an effective $V(\Omega_m) \propto 1/|\Omega_m|^{\gamma}$; the corresponding $\Sigma(\omega_m) \propto |\omega_m|^{1-\gamma}$. Equation (7) corresponds to $\gamma = 1/2$.

2. Pairing of lukewarm fermions

Subsequent studies [3,30], however, have found that the threshold at ϵ_c is actually a crossover rather than a sharp boundary, i.e., T_c is finite even when ϵ is small. The argument is that lukewarm fermions in Eq. (5) also contribute to pairing. Because these fermions display a Fermi-liquid behavior, it seems natural to expect that the pairing of lukewarm fermions falls into the BCS framework. Indeed, T_c, obtained in Ref. [3], remains finite even at the smallest ϵ and has a familiar BCS form

$$T_c \sim \omega_0 e^{-1/\epsilon}. \tag{8}$$

We show below that the analogy with BCS is deceptive. Namely, while there is no threshold, the pairing mechanism is still qualitatively different from BCS. In particular, we show that there is a tower of $T_{c,n}$ of which the one in Eq. (8) is the largest.

The gap equation for lukewarm fermions is obtained from (6) by using the self-energy from (5) and neglecting the dynamical Landau damping term in the bosonic propagator, which is smaller than the static term for frequencies and momenta, relevant to pairing, as one can verify *a posteriori*. To see this, we focus on the lukewarm regime ($\gamma \omega'_m \ll k_\parallel'^2$) in the integral of Eq. (6) and drop the ω'_m dependence in the bosonic propagator. From the remaining terms in the bosonic propagator, we obtain that the pairing vertex in different regimes of $(k_\parallel, \omega_m)$ is described by a single-variable function:

$$\Phi(k_\parallel, \omega_m) = \begin{cases} \Phi(k_\parallel^2/\gamma) & \text{if } k_\parallel^2 \gg \gamma \omega_m, \\ \Phi(\omega_m) & \text{if } k_\parallel^2 \ll \gamma \omega_m. \end{cases} \tag{9}$$

Plugging this into the right-hand side of Eq. (6), we obtain

$$\Phi(k_\parallel^2/\gamma) = \frac{\epsilon}{\pi} \int_{\gamma T}^{\gamma \omega_0} \frac{dk_\parallel'^2}{k_\parallel^2 + k_\parallel'^2} \log(k_\parallel'^2/\gamma T) \Phi(k_\parallel'^2/\gamma)$$
$$+ \frac{\epsilon \alpha \lambda}{\pi v_F} \int_T^{\omega_0} \frac{d\omega'_m}{k_\parallel^2 + \gamma \omega'_m} \int_0^{\sqrt{\gamma \omega'_m}} \frac{dk_\parallel'}{\sqrt{\omega_0 \omega'_m}} \Phi(\omega'_m), \tag{10}$$

where $\alpha = O(1)$. For small ϵ, the contribution from the first line is the largest one. Keeping only this term and introducing $x = k_\parallel^2/\gamma T$ and $y = k_\parallel'^2/\gamma T$ in the top line of Eq. (10), we obtain

$$\Phi(x) = \frac{\epsilon}{\pi} \int_1^{\omega_0/T} \frac{dy}{x+y} \log(y) \Phi(y). \tag{11}$$

The $1/(x+y)$ on the right-hand side of this equation is the static part of the spin-mediated interaction in rescaled variables, and the $\log(y)$ term is the Cooper logarithm from lukewarm fermions, which, we remind the reader, display a Fermi liquid behavior.

III. DIFFERENTIAL GAP EQUATION

A convenient way to analyze this equation, applied before to dynamical pairing out of a non-Fermi-liquid and to pairing near a van Hove point in a metal [29,31,40], is to convert the integral equation into a differential one, which is easier to analyze. For our case, the conversion is done by approximating $1/(x+y)$ in Eq. (11) by $1/x$ when $x > y$ and by $1/y$ when

$y > x$. This is known as the local approximation [31,40]. It is quantitatively exact if the interaction $V(l)$ is a slow function of the variable l. In our case, the interaction $V(l) \propto 1/l$ is not particularly slow, yet we shall see that the differential gap equation (DGE) remains qualitatively valid.

Applying this, we obtain from (11)

$$\Phi(x) = \frac{\epsilon}{\pi} \left[\frac{1}{x} \int_1^x dy \log(y) \, \Phi(y) + \int_x^{\frac{\omega_0}{T}} \frac{dy \log(y)}{y} \, \Phi(y) \right]. \tag{12}$$

For x well above the lower limit, the second term scales as $\log^2 x$ and the first as $\log x$. It is then tempting to only keep the second term and drop the first one. Imposing this, we obtain from (12)

$$\Phi(x) = \frac{\epsilon}{\pi} \int_x^{\omega_0/T} \frac{dy \log(y)}{y} \Phi(y). \tag{13}$$

Differentiation over x then yields a local differential equation

$$\Phi'(x) = -\frac{\epsilon}{\pi} \frac{\log(x)}{x} \Phi(x). \tag{14}$$

The boundary condition is set by (13)

$$\Phi\left(\frac{\omega_0}{T}\right) = 0. \tag{15}$$

Solving (14), we obtain

$$\Phi(x) = \Phi_0 \exp\left[-\frac{2\epsilon}{\pi} \log^2 x \right]. \tag{16}$$

Indeed, this is the result of summing the perturbative series in terms of the $\log^2 x$ term [3]. However, this function does not satisfy the boundary condition (15) at any T. This implies that the summation of the leading logarithms does not lead to an instability. This already shows that the pairing of lukewarm fermions is different from BCS. In Appendix A we further contrast this with color superconductivity, where the gap equation has a similar form, yet the summation of the leading logarithms gives rise to a finite T_c.

We now return to the full Eq. (12) and keep both terms on the right-hand side. One can easily verify that to obtain a local differential equation, one has to differentiate twice. Indeed, differentiating once, we obtain

$$\Phi'(x) = -\frac{\epsilon}{\pi x^2} \int_1^x dy \log(y) \, \Phi(y) = 0. \tag{17}$$

Differentiating again, we obtain

$$\Phi''(x) + \frac{2}{x} \Phi'(x) + \frac{\epsilon}{\pi} \frac{\log(x)}{x^2} \Phi(x) = 0. \tag{18}$$

The two boundary conditions can be extracted from the original equation (12) and from Eq. (17). They are

$$\Phi'(1) = 0,$$
$$\Phi'\left(\frac{\omega_0}{T}\right) + \frac{T}{\omega_0} \Phi\left(\frac{\omega_0}{T}\right) = 0. \tag{19}$$

A. Approximate differential equation

As a first step in the analysis, let us consider an approximate (toy-model) version of Eq. (18) in which we assume that

relevant x are of order the upper limit $x \sim \omega_0/T$, at least to logarithmic accuracy, and we replace $\log(x)$ on the right-hand side of (18) by $\log(\omega_0/T)$. The differential equation then becomes

$$\Phi''(x) + \frac{2}{x}\Phi'(x) + \frac{D}{x^2}\Phi(x) = 0, \qquad (20)$$

where

$$D = \frac{\epsilon}{\pi} \log\left(\frac{\omega_0}{T}\right) \qquad (21)$$

is the T-dependent parameter. At large $T \leqslant \omega_0$, D is small, of order ϵ. At the smallest T, D becomes large.

The solution of (20) is a simple power-law function, which we choose as $\Phi(x) \propto x^{\beta - 1/2}$. Substituting into (20), we obtain the equation on β:

$$\beta^2 + D - \frac{1}{4} = 0, \qquad (22)$$

whose solution is $\beta_{1,2} = \pm\sqrt{1/4 - D}$. At $D < 1/4$ (larger T), β is real. The generic solution of (20) is then

$$\Phi(x) = \frac{\Phi_0}{\sqrt{x}}\left(\frac{1}{x^\beta} + Cx^\beta\right). \qquad (23)$$

Substituting into the boundary condition (19) at $x = 1$, we fix C to be $C = -(1/2 - \beta)/(1/2 + \beta)$. However, the second boundary condition is not satisfied for any positive β. This implies that there is no nonzero solution of (20) when $D < 1/4$.

At $D > 1/4$, β becomes imaginary $i\tilde{\beta}$, where $\tilde{\beta} = \sqrt{D - 1/4}$. A generic solution of (20) now becomes

$$\Phi(x) = \frac{\Phi_0}{\sqrt{x}}\cos(\tilde{\beta}\log(x) + \phi), \qquad (24)$$

where ϕ is a free parameter. Substituting this $\Phi(x)$ into the two boundary conditions in (19), we find from the condition at $x = 1$, $\tan\phi = -1/(2\tilde{\beta})$, and from the one at $x = \omega_0/T$,

$$\tan\left[\tilde{\beta}\log\left(\frac{\omega_0}{T}\right) + \phi\right] - \frac{1}{2\tilde{\beta}} = 0. \qquad (25)$$

Using $\tilde{\beta} = \sqrt{D - 1/4}$, Eq. (21) for D, and the first boundary condition, we reexpress Eq. (25) as

$$\tan\left(\sqrt{4D - 1}\frac{\pi D}{2\epsilon}\right) - \frac{\sqrt{4D - 1}}{2D - 1} = 0. \qquad (26)$$

The graphical solution of (26) is shown in Fig. 2. We see that there are an infinite number of solutions $T_{c,n}$. At small ϵ, the solutions are closely packed. The largest T_c corresponds to $D \approx 1/4$,[5] and is given by

$$T_{c,0} = T_c \sim \omega_0 \exp\left(-\frac{\pi}{4\epsilon}\right). \qquad (27)$$

This T_c is almost the same as in (8) except for the factor $\pi/4$ in the exponent.

We see from this analysis that while there is no threshold for T_c, and T_c depends exponentially on ϵ, like in BCS theory, other features are qualitatively different from BCS. Namely,

---

[5]$D = 1/4$ is formally also a solution of Eq. (26), but it corresponds to a trivial pairing vertex $\Phi(x) = 0$.

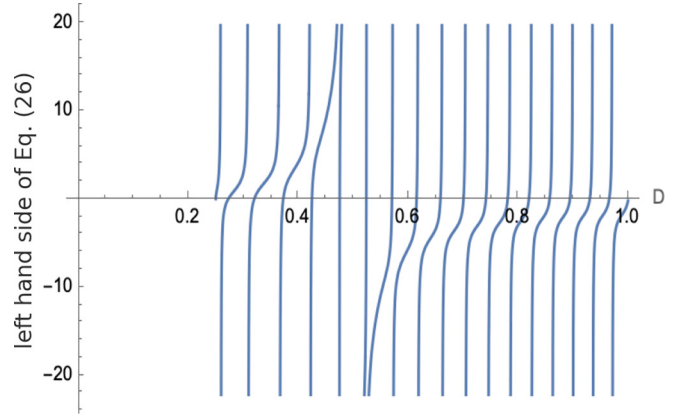FIG. 2. Solutions for D in Eq. (26) for $\epsilon = 0.05$, represented by the zeros of the curve. For $\epsilon \ll 1$, the first solution is at $D \approx 1/4$.

the pairing instability does not emerge from the summation of the leading logarithms, but rather falls into the "complex exponent" category. In addition, there is a tower of $T_{c,n}$ for different pairing states.

B. Full differential equation

We now show that very similar results hold in the original differential equation (18) without approximating $\log x$ by $\log(\omega_0/T)$. To this end, it is instructive to reexpress the derivative over x into the one over $L \equiv \log(x)$. Doing this, we obtain from (18)

$$\frac{d^2\Phi}{dL^2} + \frac{d\Phi}{dL} + \frac{\epsilon L}{\pi}\Phi = 0. \qquad (28)$$

The first-order derivative above can be removed by defining $\varphi(L) \equiv e^{L/2}\Phi(L)$. The equation for the new function $\varphi(L)$ takes the form of the Airy equation,

$$\varphi''(L) + \left(\frac{\epsilon}{\pi}L - \frac{1}{4}\right)\varphi(L) = 0. \qquad (29)$$

The solution for $\varphi(x)$ can then be straightforwardly expressed as

$$\varphi(L) = C_1\,\mathrm{Ai}(z) + C_2\,\mathrm{Bi}(z),$$
$$\text{where } z = \frac{1}{4}\left(\frac{\pi}{\epsilon}\right)^{2/3} - \left(\frac{\epsilon}{\pi}\right)^{1/3}L, \qquad (30)$$

and Ai and Bi are Airy functions of the first and second kind. Then

$$\Phi(L) = e^{-L/2}[C_1\,\mathrm{Ai}(z) + C_2\,\mathrm{Bi}(z)]. \qquad (31)$$

The boundary conditions for $\Phi(L)$ are

$$\Phi'(0) = 0, \quad \Phi'\left(\log\frac{\omega_0}{T}\right) = -\Phi\left(\log\frac{\omega_0}{T}\right), \qquad (32)$$

where the derivatives are over L. In the limit $\epsilon \ll 1$, using the asymptotic behavior [41] of the Airy functions that $\mathrm{Ai}'(z)/\mathrm{Ai}(z) \sim -\sqrt{z}$ for $z \gg 1$, we find that the boundary condition $\Phi'(0) = 0$ is satisfied by choosing $C_2 = 0$. The other boundary condition in Eq. (32) yields

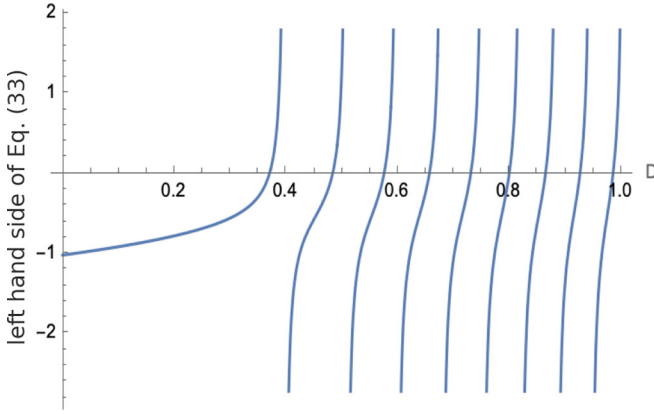$$\left(\frac{\epsilon}{\pi}\right)^{1/3}\frac{\mathrm{Ai}'(z_D)}{\mathrm{Ai}(z_D)} - \frac{1}{2} = 0, \qquad (33)$$

FIG. 3. Solutions of Eq. (33) for $\epsilon = 0.05$ in terms of D. For small $\epsilon \ll 1$, the leading T_c corresponds to $D \approx 1/4$.
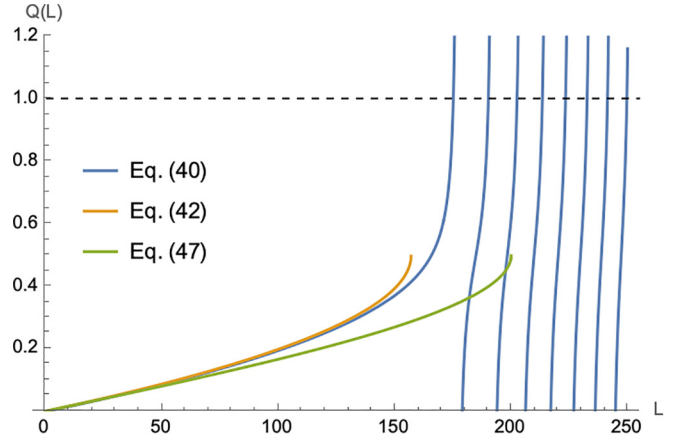

FIG. 4. Solutions for $Q(L)$ using DGE and an algebraic equation with and without improvements beyond the local approximation. The boundary condition in Eq. (39) is shown as a dashed line.

where

$$z_D = \frac{1}{4}\left(\frac{\pi}{\epsilon}\right)^{2/3} - \left(\frac{\epsilon}{\pi}\right)^{1/3} \log\frac{\omega_0}{T} = -\left(\frac{\pi}{\epsilon}\right)^{2/3}\left(D - \frac{1}{4}\right). \tag{34}$$

We find the solution of (33) graphically in Fig. 3. As can be seen, this boundary condition is satisfied at various values of $D > 1/4$, corresponding to a tower of $T_{c,n}$'s. Indeed, from the property of the Airy function [41], the left-hand side of (33) is oscillatory for $D > 1/4$ and monotonically negative for $D < 1/4$. For $\epsilon \ll 1$, the largest $T_{c,0}$ corresponds to $D \approx 1/4$, and thus

$$T_{c,0} = T_c \sim \omega_0 \exp\left(-\frac{\pi}{4\epsilon}\right). \tag{35}$$

We see that the functional form is the same as in (27). However, the subleading terms in the expansion in ϵ are different.

In the original variable x, the exact solution for $\Phi(x)$ is

$$\Phi(x) = \frac{\Phi_0}{\sqrt{x}} \text{Ai}\left[\frac{1}{4}\left(\frac{\pi}{\epsilon}\right)^{2/3} - \left(\frac{\epsilon}{\pi}\right)^{1/3} \log x\right]. \tag{36}$$

We remind the reader that this solution exists only when $D > 1/4$. Observe that Eq. (36) is similar to Eq. (24).

For subsequent analysis, it is convenient to introduce the new function

$$Q(L) = -\frac{d \log \Phi(x)}{d \log x}. \tag{37}$$

The DGE for $Q(L)$ has the form

$$Q'(L) = Q^2(L) - Q(L) + \frac{\epsilon}{\pi} L, \tag{38}$$

and the boundary conditions are

$$Q(0) = 0, \quad Q\left(\log\frac{\omega_0}{T}\right) = 1. \tag{39}$$

Equation (38) is known as a Riccati equation. Using (31), we obtain its solution,

$$Q(L) = \frac{1}{2} + \left(\frac{\epsilon}{\pi}\right)^{1/3} \frac{\text{Ai}'(z)}{\text{Ai}(z)}. \tag{40}$$

The boundary conditions Eq. (39) yield the same tower of T_c as Eq. (33).

C. Computing T_c via an algebraic equation for Q

We now show that for small ϵ, the formulas for $T_{c,0}$ and $\Phi(x)$, consistent with (35) and (36), can be obtained from (38) in a purely algebraic way, without solving the differential equation. For this we note that at $\epsilon \ll 1$, Q' remains small compared to Q and Q^2 in nearly the whole range of $L < \pi/(4\epsilon)$, except very close to the boundary of this range. Within this range, the DGE (38) can be approximated by a quadratic algebraic equation

$$Q^2(L) - Q(L) + \frac{\epsilon}{\pi} L = 0, \tag{41}$$

whose solution is

$$Q(L) = \frac{1 - \sqrt{1 - 4\epsilon L/\pi}}{2}, \tag{42}$$

which we plot in Fig. 4. We see that the approximation of (40) by (42) is quite good for $L < \pi/(4\epsilon)$. The other quadratic root does not satisfy the boundary condition $Q(0) = 0$. This solution is valid up to $4\epsilon L/\pi < 1$. To leading order of ϵ at a given L, this gives

$$Q(L) \approx \frac{\epsilon L}{\pi}. \tag{43}$$

The corresponding

$$\Phi(x) = \Phi_0 \exp\left[-\frac{2\epsilon}{\pi} \log^2 x\right] \tag{44}$$

is the same as in (16), i.e., the approximation to linear order in ϵ for $Q(L)$ is equivalent to solving for $\Phi(x)$ within the leading logarithmic approximation. The function $Q(L)$ from (43) increases with L, but reaches $Q = 1/4$ at the maximal $L = \pi/(4\epsilon)$ and then does not satisfy the second boundary condition $Q(L = \log(\omega_0/T)) = 1$. This is a different way to state that the summation of the leading logarithms in the gap equation does not lead to the pairing susceptibility.

The full algebraic solution for $Q(L)$ also does not satisfy the boundary condition $Q(L = \log(\omega_0/T)) = 1$ as its maximum value is $1/2$. However, there is an important difference with $Q(L)$ from (43). Namely, $Q(L)$ from (42) nearly coincides with the exact solution of the DGE for all $L <$

$\pi/(4\epsilon)$ except the ones very close to $\pi/(4\epsilon)$ (see Fig. 3), and, moreover, its derivative diverges at $L \to \pi/(4\epsilon)$. Judging from this alone, one can conclude that the full solution of the DGE for $Q'(L)$ should cross $Q(L) = 1$ at L only slightly above $L = \pi/(4\epsilon)$. To find out how this happens, one indeed should keep $Q'(L)$ in the DGE, as Fig. 3 shows. However, this reasoning already implies that to leading order in ϵ, $T_c = T_{c,0}$ can be extracted from the condition $\log(\omega_0/T_c) = \pi/(4\epsilon)$. This yields the same T_c as in (35). We note, however, that within this reasoning, one cannot obtain the tower of $T_{c,n}$.

D. Improved equation for Q

We now stay within the regime of L where $Q' \ll Q, Q^2$, and we address another issue—how accurate is the computational procedure leading to the algebraic equation (41)? We remind the reader that in the derivation of this equation, we used the local approximation and replaced $1/(x+y)$ in the kernel in Eq. (11) by $1/\max(x, y)$. We now argue that the local approximation can be improved, at least in the regime where Q' is smaller than Q^2 and Q and can be neglected. To this end, note that from the definition of Q, $\Phi(y)$ at a given y can be expressed via $\Phi(x)$ as some x as

$$\Phi(y) = \Phi(x) \exp[-Q(\log x)(\log y - \log x)], \quad (45)$$

where higher-order derivative terms, such as $Q'(\log y)|_{y=x}$, have been dropped. Inserting this relation into the original integral equation (11), we get

$$
x^{-Q(\log x)} = \frac{\epsilon}{\pi} \int_1^x \frac{y^{-Q(\log x)}}{x+y} \log y \, dy + \frac{\epsilon}{\pi} \int_x^{\frac{2}{T}} \frac{y^{-Q(\log x)}}{y+x} \log y \, dy
$$
$$
= \frac{\epsilon}{\pi} \sum_{n=1}^{\infty} \frac{(-1)^{n-1}}{x^n} \int_1^x y^{n-1-Q(\log x)} \log y \, dy + \frac{\epsilon}{\pi} \sum_{n=1}^{\infty} (-1)^{n-1} x^{n-1} \int_x^{\frac{2}{T}} y^{-n-Q(\log x)} \log y \, dy, \quad (46)
$$

where in the second line we expanded the kernel in y and x, respectively. Only keeping the $n = 1$ contribution in both terms amounts to taking the local approximation, which, after performing the integrals, reproduces Eq. (41). We go beyond the local approximation by retaining all terms in the sums. Evaluating the integrals and performing the resummation, we obtain a more accurate equation for $Q(L)$ in the form

$$
1 = \frac{\epsilon}{\pi} \left[\sum_{n=-\infty}^{\infty} \frac{(-)^{n+1}}{n - Q(L)} \right] L = \frac{\epsilon L}{\sin[\pi Q(L)]}. \quad (47)
$$

We plot the solution of this equation in Fig. 4. We see that the solution gets modified from Eq. (42) at larger L's, but still only exists in a limited range of L, and does not reach $Q(L) = 1$ at the boundary of this range. Yet, the solution of (47) rapidly increases at the edge of its applicability range, much like the solution of (42). By analogy, it is reasonable to expect that the largest L, where the solution of (47) holds, is close to $\log \omega_0/T_c$. We see that, in distinction to the solution of (42), the largest L up to which the solution of (47) holds is $L = 1/\epsilon$. We then obtain an improved estimate for T_c as

$$
T_c \sim \omega_0 \exp\left(-\frac{1}{\epsilon}\right). \quad (48)
$$

This is the result that we cited in the Introduction. The formula for T_c looks like the BCS formula, yet, as we demonstrated, the pairing mechanism is not BCS—it falls into the "complex exponent" rather than the "Cooper logarithm" category, and there is a tower of $T_{c,n}$ with topologically distinct $\Phi_n(x)$, similar to pairing out of a non-Fermi-liquid. The only distinction from the latter is the absence of the threshold for the coupling, which results from the coherent Fermi-liquid behavior of lukewarm fermions.

Equation (48) was first obtained by us in Ref. [3] and was found to match numerics quite well. In that paper, however, we did not explore the fact that one needs to keep Q' in the DGE in order to satisfy the boundary condition $Q(\log(\omega_0/T)) = 1$, and we did not emphasize the non-BCS nature of the pairing of lukewarm fermions. It is tempting to further improve the DGE by incorporating Q' terms into Eq. (47). This, however, requires rather sophisticated calculations outside of the local approximation. We leave this issue for future work.

IV. RG FORMULATION OF THE PAIRING PROBLEM AND ITS RELATION TO DGE

In this section, we reformulate the pairing problem using the technique of momentum-shell RG, and we show that it is fully equivalent with the differential equation.

Within the BCS pairing mechanism, under the RG flow toward the FS, the tangential component of momentum $k_{\parallel}$ does not rescale [42,43]. However, in our problem, since the self-energy for lukewarm fermions explicitly depends on $k_{\parallel}$, it is crucial that $k_{\parallel}$ also rescales under RG. Given the form of the self-energy, we employ an RG scheme with the following scaling dimensions:

$$
[k_{\parallel}] = \tfrac{1}{2}, \quad [k_{\perp}] = \tfrac{1}{2}, \quad [\omega] = 1. \quad (49)
$$

As the instability arises from integrating over $k_{\parallel}$, we implement a momentum-shell RG process during which at each step, (i) modes in a momentum shell $k_{\parallel}^2 \in (\Lambda(1 - D\ell), \Lambda)$ are integrated out, and then (ii) the upper cutoff is formally rescaled back to Λ.

As an immediate consequence of $[k_{\parallel}] \neq 0$, the engineering dimension of the pairing coupling g is altered. Unlike the BCS pairing mechanism in which g is marginal [42,43], here g is irrelevant, and by a similar analysis to that in Ref. [43], we get

$$
[g] = -1. \quad (50)
$$

At each RG step, the scaling dimension of g leads to

$$\delta_1 g = -g \delta\ell. \qquad (51)$$

There are two additional fundamental differences with the BCS pairing mechanism. First, the coupling "constant" g is not a constant, but rather by itself is a function of $k_\parallel$, i.e., explicitly scale-dependent. As a common feature in all quantum-critical pairing models, the standard treatment within the RG [1,8] is to identify g with the pairing interaction at a given running scale Λ. This is equivalent to the local approximation, and it is strictly speaking accurate (to log accuracy) if the pairing interaction is slowly varying at log scale. This is satisfied by the γ-model at small γ and color superconductivity in $3 + 1$D. In our case, the pairing interaction $D(k_\parallel) \sim \epsilon/(\pi k_\parallel^2)$, and such treatment is not quantitatively accurate. Still, as we shall see, it correctly captures the qualitative feature of the pairing mechanism. The local approximation leads to an inherent running of g aside from regular contributions from the RG procedure. This leads to, during an RG step $\Lambda \to \Lambda(1 - \delta\ell)$,

$$\delta_2 g = \frac{\epsilon}{\pi} \frac{\delta\ell}{\Lambda}. \qquad (52)$$

Second, the one-loop contribution to the running of g is also different from BCS. In BCS, the one-loop contribution to the RG flow comes from a shell of $(k_\perp, \omega)$ with $k_\parallel$ integrated over. Here, $k_\parallel$ is the running scale. In a momentum shell $k_\parallel^2 \in (\Lambda(1 - \delta\ell), \Lambda)$, the contribution to one-loop pairing susceptibility is

$$g^2 \int_{\Lambda(1-\delta\ell)}^{\Lambda} dk_\parallel^2 \int_{Te^\ell}^{k_\parallel^2} \frac{d\omega}{\omega}. \qquad (53)$$

Note that the lower cutoff of the frequency integral is rescaled to Te^ℓ instead of T, due to the substeps (ii) during the RG flow ($\ell = \int \delta\ell$). This leads to a change in g given by

$$\delta_3 g = g^2 \Lambda \left(\log \frac{\Lambda}{T} - \ell \right) \delta\ell. \qquad (54)$$

Combining Eqs. (51), (52), and (54), we get the following β-function for the RG flow of g:

$$\frac{dg}{d\ell} = \frac{\epsilon}{\pi\Lambda} - g + g^2 \Lambda \left(\log \frac{\Lambda}{T} - \ell \right). \qquad (55)$$

The RG flow begins at the UV scale $\Lambda = \omega_0$ and stops at $\ell = \log(\omega_0/T)$. For the pairing instability at $T = T_c$, we have the boundary conditions

$$g(\ell = 0) = \frac{\epsilon}{\pi\Lambda}, \quad g\left(\ell = \log \frac{\omega_0}{T}\right) \to \infty. \qquad (56)$$

Remarkably, if one identifies L in (38) with the "reverse RG time," and Q with the "inverse coupling" [31], i.e.,

$$L \leftrightarrow \log \frac{\Lambda}{T} - \ell, \quad Q(L) \leftrightarrow \frac{\epsilon\Lambda}{\pi g(\ell)}, \qquad (57)$$

the RG equation (55) becomes exactly the same as the DGE, Moreover, the boundary conditions for g in Eq. (56) precisely map to those for Q in Eq. (39).

For a number of pairing problems, it is known that the approaches of the Eliashberg equation and the RG are equivalent [1,31]. In particular, for pairing mediated by dynamic interactions, Ref. [31] showed explicitly that the differential equation converted from the Eliashberg integral equation can be directly mapped to an RG equation. For the present problem, the pairing interaction is predominantly static, but the relation between $\Phi(k_\parallel)$ and $g(\ell)$ still holds. For completeness, in Appendix A we explicitly demonstrate that for color superconductivity mediated by massless gluons and for the γ-model, the RG equations and the differential equations from Eliashberg equations are exactly the same.

The derivation of the RG equation makes clear the fundamental difference between our pairing mechanism and BCS. For the BCS mechanism, the RG equation is simply

$$\frac{dg}{d\ell} = g^2, \qquad (58)$$

in which the fermionic self-energy and the form of the pairing interaction do not play an important role.

The last term in Eq. (55) is quite similar to the RG equation for pairing in graphene at van Hove doping [44], whose one-loop pairing susceptibility contains $\log^2$ just like our problem. Had we only kept this term, solving the RG equation would yield $T_c = \omega_0 \exp(-\sqrt{2/\epsilon})$, quite like that for van Hove doped graphene [44] and for color superconductivity [1,45] (see Appendix A 1). However, the additional terms in the RG equation lead to a different, BCS-like formula for T_c, in spite of a fundamentally different pairing mechanism.

Compared with the RG equation for the γ-model [8] (see Appendix A 2), the first two terms in Eq. (55) are similar. The only difference is the additional L factor in the last term. As a direct consequence, there is no fixed point at $\ell \to \infty$ for an arbitrarily small ϵ, i.e., our pairing problem does not have a threshold for pairing strength.

V. CONCLUSIONS

In this work, we argued that the very appearance of the BCS-looking formula for superconducting T_c does not necessarily imply a BCS pairing mechanism, rooted in the geometric series of Cooper logarithms. We considered as an example the pairing of lukewarm fermions in the critical spin-fermion model. These fermions are located near hot spots, but still at some distance from them, and their self-energy has a Fermi-liquid form, but $d\Sigma(\omega, k)/d\omega \propto 1/|k_\parallel|$, where $k_\parallel$ is the distance of a lukewarm fermion from a hot spot. We showed using several computational procedures, with varying degrees of accuracy, that lukewarm fermions pair already for arbitrarily weak attraction ϵ, and the corresponding T_c is exponential in $1/\epsilon$, as in BCS theory. At first glance, this looks like BCS pairing. However, we demonstrated that the pairing mechanism is qualitatively different from BCS in three aspects: (i) the summation of the leading logarithms does not lead to pairing, (ii) pairing occurs in subleading terms and develops when the exponent for the pairing susceptibility becomes complex, and (iii) there is an infinite set of critical temperatures for topologically distinct gap functions. All three properties are characteristics of fundamentally non-BCS pairing. From a field-theoretic perspective, the distinction between the present pairing mechanism and BCS is rooted in their qualitatively different pairing coupling constant behaviors under RG flow.

DATA AVAILABILITY

The data are available from the authors upon reasonable request.

APPENDIX A: EQUIVALENCE BETWEEN DGE AND RG EQUATION FOR THE RUNNING COUPLING

In this Appendix, we analyze the connection between the differential equation for the pairing vertex and the RG equation for the running coupling. A differential equation for the pairing vertex is obtained from the original integral Eliashberg equation for the pairing vertex by taking the local approximation, which simplifies the pairing interaction $V(a-b)$, where a and b are external and internal variables (momentum or frequency), to $V(a)$ for $a > b$ and $V(b)$ for $b > a$, and the RG equation for the coupling is obtained by using a Wilsonian coarse-graining procedure with the convention that the RG coupling has to diverge at the energy scale set by T_c.

A generic analysis of the interplay has been performed in Ref. [31], where the authors demonstrated that for a generic dynamical interaction $V(a-b)$, T_c extracted from the differential equation and from RG are equivalent.

We focus on two specific examples: color superconductivity (pairing by a logarithmically singular dynamical interaction) and the pairing by the effective dynamical interaction $V(\Omega_m) \propto 1/|\Omega_m|^\gamma$ (the γ model). For both cases, we present the explicit expressions for the differential equation and its solution, and we convert the equation for the pairing vertex Φ into the one for the RG coupling g.

1. Color superconductivity

Color superconductivity occurs in quark matter due to condensation of quark pairs (diquarks) driven by logarithmically singular attractive interactions mediated by gluon exchange [1]. Despite its exotic nature, the same pairing mechanism can also be realized in electronic pairing, as long as the pairing interaction is logarithmically singular (e.g., interaction mediated by nematic fluctuations in three dimensions). The instability temperature for color superconductivity was found by Son within the RG framework [1] (see also Ref. [24,26]). Chubukov and Schmalian [45] reproduced Son's result for T_c by constructing the Eliashberg equation for the pairing vertex with a source term (an integral equation in frequency) and analyzing the pairing susceptibility.

The point of departure for our analysis is the integral Eliashberg equation in Matsubara frequencies, without the source term. For logarithmic interaction, it has the form

$$\Phi(x) = \lambda \int_{\bar{T}}^1 \frac{dy}{y} \log\left(\frac{1}{|x-y|}\right)\Phi(y), \tag{A1}$$

where $x, y > 0$ are rescaled frequencies $x = \omega_m/\Lambda$, where Λ is the upper cutoff for logarithmical behavior of the interaction, $\bar{T} = T/\Lambda$, and λ is a dimensional coupling, which we assume to be small.

The differential equation corresponding to (A1) is obtained using the same procedure as in the main text. It is

$$\Phi''(x) + \frac{\Phi'(x)}{x} + \lambda\frac{\Phi(x)}{x^2} = 0, \tag{A2}$$

and the boundary conditions are

$$\Phi(x=1) = 0, \quad \Phi'(x=\bar{T}) = 0. \tag{A3}$$

The solution of (A2) is a power law, $\Phi(x) \propto x^\beta$. Substituting into (A2), one finds that $\beta = \pm i\sqrt{\lambda}$ is imaginary for any nonzero λ. Accordingly,

$$\Phi = \Phi_0 \cos\left[\sqrt{\lambda}\log\left(\frac{1}{x}\right) + \phi\right], \tag{A4}$$

where ϕ is a free parameter. Substituting into (A3), we find $\phi = \pi/2$ and

$$\sqrt{\lambda}\log\left(\frac{1}{\bar{T}}\right) = \frac{\pi}{2}(1+2n). \tag{A5}$$

Hence

$$T_{c,n} \sim \Lambda \exp\left[-\frac{\pi(1+2n)}{2\sqrt{\lambda}}\right]. \tag{A6}$$

Analyzing the solution, we find that the case of color superconductivity is an intermediate between BCS and non-BCS pairing and has features of both. As in the BCS case, the pairing comes from the summation of the leading logarithms (series of $\log^2$ terms), and T_c is exponential in $1/\sqrt{\lambda}$. As in the non-BCS case, the pairing instability is associated with the complex exponent in the power-law solution for $\Phi(x)$, and there is a tower of $T_{c,n}$ for topologically distinct $\Phi_n(x)$ with n zeros on a positive Matsubara semiaxis.

We now demonstrate how to convert Eqs. (A2) and (A3) into the equation for the running coupling g that departs from a constant at $x = 1$ and diverges at $x = \bar{T}$. For this we follow the analysis in Sec. IV of the main text and introduce $p = \log 1/x$ and $Q = -d(\log \Phi(x))/d\log(x) = d(\log \Phi(p))/dp$. Reexpressing (A2) as the equation on $Q(p)$, we find

$$Q'(p) + Q^2(p) + \lambda = 0, \tag{A7}$$

where the derivative is with respect to p, and p is running between $p_{\min} = 0$ and $p_{\max} = \log(\omega_0/T)$. The boundary conditions are

$$Q(p_{\min}) = \infty, \quad Q(p_{\max}) = 0. \tag{A8}$$

Introducing then $g(p) = 1/Q(p)$, we finally obtain

$$g'(p) = 1 + \lambda g^2 \tag{A9}$$

with the boundary conditions

$$g(p_{\min}) = 0, g(p_{\max}) = \infty. \tag{A10}$$

This coincides with the equation for RG coupling, obtained by Son [1]. Solving (A9) and using (A10), one obtains

$$g(p) = \frac{1}{\sqrt{\lambda}} \tan{(\sqrt{\lambda} p)} \qquad (A11)$$

subject to $\cos{(\sqrt{\lambda} p_{\max})} = 0$. This leads to the same tower of $T_{c,n}$ as in (A6).

2. γ-model

We now apply the same reasoning to the pairing in the γ-model [2,11,13], which describes a set of quantum-critical models with the effective interaction $V(\Omega_m) \propto 1/|\Omega_m|^\gamma$ and normal state self-energy $\Sigma(\omega_m) = |\omega_m|^{1-\gamma} \omega_0^\gamma \operatorname{sgn}(\omega_m)$, where ω_0 is a function of the coupling between fermions and a critical boson.

As before, we use the integral gap equation in frequency as the point of departure of our analysis. It has been presented and discussed in Refs. [28,40], where the authors also analyzed the full corresponding differential equation.

For our purpose of comparing with RG, it is sufficient to set the lower limit of frequency integration at T and the upper one at ω_0 and neglect bare ω compared to the self-energy. We also restrict to $\gamma < 1$. The truncated Eliashberg equation is

$$\Phi(x) = \lambda \int_{\bar{T}}^1 \frac{dy}{|x-y|^\gamma} \frac{\Phi(y)}{y^{1-\gamma}}, \qquad (A12)$$

where, as before, $x, y > 0$ are frequencies in units of ω_0, $\bar{T} = T/\omega_0$, and λ is a dimensional coupling related to the ratio of fully dressed interactions in the particle-particle and particle-hole channels [in the extended matrix SU(N) model with $N \gg 1$, $\lambda \propto 1/N$ [5,12]]. Converting Eq. (A12) into the differential equation in the same way as in the main text and introducing $z = x^\gamma$, we obtain

$$\Phi''(z) + \frac{2}{z}\Phi'(z) + \frac{\lambda}{\gamma}\frac{\Phi(z)}{z^2} = 0 \qquad (A13)$$

with the boundary conditions being

$$\Phi'(1) + \Phi(1) = 0, \quad \Phi'(z = \bar{T}^\gamma) = 0. \qquad (A14)$$

The derivatives are with respect to z. The solution is again a power-law $\Phi(z) \propto z^{\beta - 1/2}$ ($-1/2$ is added to simplify formulas below). Substituting into (A13), one obtains

$$\beta = \pm \frac{1}{2}\sqrt{1 - \frac{4\lambda}{\gamma}}. \qquad (A15)$$

For small λ, β are real. A simple experimentation shows that one cannot satisfy the two boundary conditions in (A14). (For a more detailed discussion on this issue, see Refs. [40,46].) This implies that there is no pairing instability at weak coupling.

At larger $\lambda > \lambda_c = \gamma/4$, $\beta = i\tilde{\beta}$ is imaginary ($\tilde{\beta} = 0.5\sqrt{\frac{\lambda}{\lambda_c} - 1}$). Now

$$\Phi(z) = \frac{1}{\sqrt{z}} \cos{(\tilde{\beta} \log(z) + \phi)}, \qquad (A16)$$

where ϕ is arbitrarily. Substituting into (A14), we obtain

$$\tan\phi = -\frac{1}{2\tilde{\beta}}, \quad \tan\left(\tilde{\beta} \log\frac{1}{\bar{T}^\gamma}\right) = \frac{2\tilde{\beta}}{2\tilde{\beta} - 1}. \qquad (A17)$$
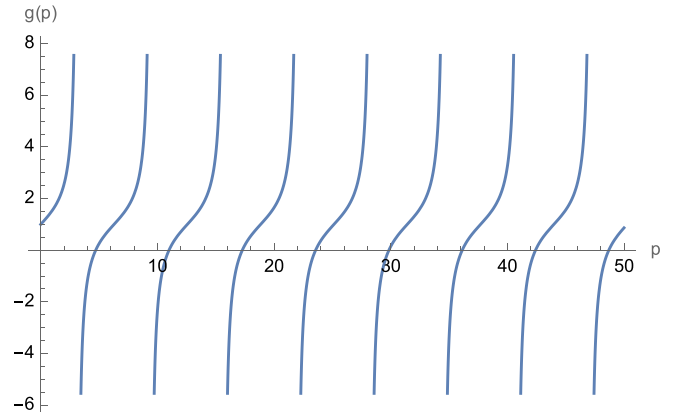

FIG. 5. The plot of $g(p)$ for $a = 2$. There is an infinite set of $p \sim \log{(\omega_0/T)^\gamma}$, at which $g(p)$ diverges.

Solving (A17) for $\lambda \geqslant \lambda_c$, we obtain a tower of critical temperatures [40],

$$T_{c,n} \sim \omega_0 \exp\left(\frac{2\pi(1+n)}{\gamma}\sqrt{\frac{\lambda_c}{\lambda - \lambda_c}}\right), \qquad (A18)$$

where $n = 0, 1, 2, \ldots$. Like before, each $T_{c,n}$ is the onset temperature for a topologically distinct $\Phi_n(z)$ with n zeros on a positive Matsubara semiaxis.

To convert (A13) into the equation for the running coupling g that departs from a constant at $z = 1$ and diverges at $z = \bar{T}^\gamma$, we again follow the analysis in Sec. IV of the main text and introduce $p = \log 1/z$ and $Q = -d(\log \Phi(z))/d\log(z) = d(\log \Phi(p))/dp$. Reexpressing (A13) as the equation on $Q(p)$, we find

$$Q'(p) + Q^2(p) - Q(p) + \frac{\lambda}{\gamma} = 0, \qquad (A19)$$

where the derivative is with respect to p, and p is running between $p_{\min} = 0$ and $p_{\max} = \log{(\omega_0/T)^\gamma}$. The boundary conditions are

$$Q(p_{\min}) = 1, \quad Q(p_{\max}) = 0. \qquad (A20)$$

Introducing as before $g(p) = 1/Q(p)$, we finally obtain

$$g'(p) = 1 - g + \frac{\lambda}{\gamma}g^2 \qquad (A21)$$

with the boundary conditions

$$g(p_{\min}) = 0, \quad g(p_{\max}) = \infty. \qquad (A22)$$

One can verify that (A10) coincides with the equation for RG coupling, derived in Ref. [8]. Solving (A21) and using (A22), one obtains

$$g(p) = \frac{2}{a}\Bigg\{1 + \sqrt{a-1}$$
$$\tan\left[\frac{1}{2}\left(\sqrt{a-1}p + 2\arctan\frac{a-2}{2\sqrt{a-1}}\right)\right]\Bigg\}, \qquad (A23)$$

where $a = \lambda/\lambda_c > 1$. This $g(p)$ is subject to $g(p = \omega_0/T^\gamma) = \infty$. We plot $g(p)$ in Fig. 5. We see that there is an infinite set of points where $g(p) = \infty$, hence a tower of $T_{c,n}$. A simple

analytical analysis shows that for $\lambda \geqslant \lambda_c$, these temperatures coincide with $T_{c,n}$ in (A18), as they should.

APPENDIX B: THE RELATION BETWEEN THE PRESENT WORK AND REF. [3]

As we said in the main text, we analyzed the pairing of lukewarm fermions back in 2013. We found a BCS-looking formula for T_c and indirectly suggested that this implies that the whole pairing problem is BCS-like. Our argument was that lukewarm fermions retain Fermi-liquid behavior even at a QCP.

In this paper, we corrected ourselves and demonstrated that the pairing problem is in fact qualitatively different from BCS. The present argument is that the self-energy of these fermions has a singular dependence on the momentum distance from a hot spot. Because of this singular dependence, the gap equation after frequency integration becomes an integral equation over momentum with a singular kernel. This, we argued, makes the pairing problem non-BCS like and similar to other problems of pairing out of a non-Fermi-liquid. However, because the singularity of the kernel is only logarithmic, the coupling, which we labeled as D [see Eq. (20)], contains the product of ϵ and $\log(\omega_0/T)$. As a signature of non-BCS pairing, the solution of the linearized gap equation exists at a nonzero threshold value D_c of order 1 (there is a tower of solutions, but let us focus here on the smallest D_c, which is still of order 1). The condition on T_c is then $\epsilon \log(\omega_0/T) = O(1)$. This yields a BCS-like formula for T_c, the same as what we obtained in Ref. [3]. However, the pairing mechanism is not BCS. We have also confirmed this by a RG analysis. We reiterate that this is a consequence of the singular momentum dependence of the self-energy for a lukewarm fermion.

[1] D. T. Son, Superconductivity by long-range color magnetic interaction in high-density quark matter, Phys. Rev. D **59**, 094019 (1999).

[2] A. Abanov, A. V. Chubukov, and A. M. Finkel'stein, Coherent vs incoherent pairing in 2d systems near magnetic instability, Europhys. Lett. **54**, 488 (2001).

[3] Y. Wang and A. V. Chubukov, Superconductivity at the onset of spin-density-wave order in a metal, Phys. Rev. Lett. **110**, 127001 (2013).

[4] M. A. Metlitski, D. F. Mross, S. Sachdev, and T. Senthil, Cooper pairing in non-fermi liquids, Phys. Rev. B **91**, 115111 (2015).

[5] A. L. Fitzpatrick, S. Kachru, J. Kaplan, S. Raghu, G. Torroba, and H. Wang, Enhanced pairing of quantum critical metals near $d = 3 + 1$, Phys. Rev. B **92**, 045118 (2015).

[6] Y.-M. Wu, A. Abanov, Y. Wang, and A. V. Chubukov, Special role of the first matsubara frequency for superconductivity near a quantum critical point: Nonlinear gap equation below t_c and spectral properties in real frequencies, Phys. Rev. B **99**, 144512 (2019).

[7] K. B. Efetov, H. Meier, and C. Pepin, Pseudogap state from quantum criticality, Nat. Phys. **9**, 442 (2013).

[8] S. Raghu, G. Torroba, and H. Wang, Metallic quantum critical points with finite BCS couplings, Phys. Rev. B **92**, 205104 (2015).

[9] Y. Wang, Solvable strong-coupling quantum-dot model with a non-fermi-liquid pairing transition, Phys. Rev. Lett. **124**, 017002 (2020).

[10] W. Jiang, Y. Liu, A. Klein, Y. Wang, K. Sun, A. V. Chubukov, and Z. Y. Meng, Monte Carlo study of the pseudogap and superconductivity emerging from quantum magnetic fluctuations, Nat. Commun. **13**, 2655 (2022).

[11] Y. Wang, A. Abanov, B. L. Altshuler, E. A. Yuzbashyan, and A. V. Chubukov, Superconductivity near a quantum-critical point: The special role of the first matsubara frequency, Phys. Rev. Lett. **117**, 157001 (2016).

[12] H. Wang, Y. Wang, and G. Torroba, Superconductivity versus quantum criticality: Effects of thermal fluctuations, Phys. Rev. B **97**, 054502 (2018).

[13] M. K.-H. Kiessling, B. L. Altshuler, and E. A. Yuzbashyan, Bounds on T_c in the Eliashberg theory of superconductivity. i: The γ-model, J. Stat. Phys. **192**, 69 (2025).

[14] I. Esterlis and J. Schmalian, Cooper pairing of incoherent electrons: An electron-phonon version of the Sachdev-Ye-Kitaev model, Phys. Rev. B **100**, 115132 (2019).

[15] Y. Wang and A. V. Chubukov, Quantum phase transition in the Yukawa-Syk model, Phys. Rev. Res. **2**, 033084 (2020).

[16] G. Pan, W. Wang, A. Davis, Y. Wang, and Z. Y. Meng, Yukawa-Syk model and self-tuned quantum criticality, Phys. Rev. Res. **3**, 013250 (2021).

[17] W. Wang, A. Davis, G. Pan, Y. Wang, and Z. Y. Meng, Phase diagram of the spin-$\frac{1}{2}$ Yukawa–Sachdev-Ye-Kitaev model: Non-fermi liquid, insulator, and superconductor, Phys. Rev. B **103**, 195108 (2021).

[18] A. Ikeda, Z. Guguchia, M. Oudah, S. Koibuchi, S. Yonezawa, D. Das, T. Shiroka, H. Luetkens, and Y. Maeno, Eliashberg equations for an electron-phonon version of the Sachdev-Ye-Kitaev model: Pair breaking in non-fermi liquid superconductors, Phys. Rev. B **101**, 174503 (2020).

[19] L. Classen and A. Chubukov, Superconductivity of incoherent electrons in the Yukawa-Syk model, Phys. Rev. B **104**, 125120 (2021).

[20] D. Valentinis, G. A. Inkof, and J. Schmalian, BCS to incoherent superconductivity crossover in the Yukawa-Sachdev-Ye-Kitaev model on a lattice, Phys. Rev. B **108**, L140501 (2023).

[21] W. Choi, O. Tavakol, and Y. B. Kim, Pairing instabilities of the Yukawa-Syk models with controlled fermion incoherence, SciPost Phys. **12**, 151 (2022).

[22] G.-A. Inkof, K. Schalm, and J. Schmalian, Quantum critical Eliashberg theory, the Sachdev-Ye-Kitaev superconductor and their holographic duals, npj Quantum Mater. **7**, 56 (2022).

[23] C. Li, D. Valentinis, A. A. Patel, H. Guo, J. Schmalian, S. Sachdev, and I. Esterlis, Strange metal and superconductor in the two-dimensional Yukawa-Sachdev-Ye-Kitaev model, Phys. Rev. Lett. **133**, 186502 (2024).

[24] C. P. Herzog, P. K. Kovtun, and D. T. Son, Holographic model of superfluidity, Phys. Rev. D **79**, 066002 (2009);

K. Jensen, A. Karch, D. T. Son, and E. G. Thompson, Holographic berezinskii-kosterlitz-thouless transitions, Phys. Rev. Lett. **105**, 041601 (2010).

[25] D. B. Kaplan, J.-W. Lee, D. T. Son, and M. A. Stephanov, Conformality lost, Phys. Rev. D **80**, 125005 (2009).

[26] V. Gorbenko, S. Rychkov, and B. Zan, Walking, weak first-order transitions, and complex CFTs, J. High Energy Phys. 10 (2018) 108.

[27] B. Hawashin, A. Eichhorn, L. Janssen, M. M. Scherer, and S. Ray, The Nordic-walking mechanism and its explanation of deconfined pseudocriticality from Wess-Zumino-Witten theory, Nat. Commun. **16**, 20 (2025).

[28] Y.-M. Wu, A. Abanov, Y. Wang, and A. V. Chubukov, Interplay between superconductivity and non-fermi liquid at a quantum critical point in a metal. ii. the γ model at a finite t for $0 < \gamma < 1$, Phys. Rev. B **102**, 024525 (2020).

[29] R. Ojajärvi, A. V. Chubukov, Y.-C. Lee, M. Garst, and J. Schmalian, Pairing at a single Van Hove point, npj Quantum Mater. **9**, 105 (2024).

[30] M. A. Metlitski and S. Sachdev, Quantum phase transitions of metals in two spatial dimensions. II. Spin density wave order, Phys. Rev. B **82**, 075128 (2010).

[31] H. Wang, S. Raghu, and G. Torroba, Non-fermi-liquid superconductivity: Eliashberg approach versus the renormalization group, Phys. Rev. B **95**, 165137 (2017).

[32] P. Monthoux, D. Pines, and G. G. Lonzarich, Superconductivity without phonons, Nature (London) **450**, 1177 (2007).

[33] D. J. Scalapino, A common thread: The pairing interaction for unconventional superconductors, Rev. Mod. Phys. **84**, 1383 (2012).

[34] A. Abanov, A. V. Chubukov, and J. Schmalian, Quantum-critical theory of the spin-fermion model and its application to cuprates: normal state analysis, Adv. Phys. **52**, 119 (2003).

[35] A. Abanov, A. V. Chubukov, and M. R. Norman, Gap anisotropy and universal pairing scale in a spin-fluctuation model of cuprate superconductors, Phys. Rev. B **78**, 220507(R) (2008).

[36] S.-S. Lee, Recent developments in non-fermi liquid theory, Annu. Rev. Condens. Matter Phys. **9**, 227 (2018).

[37] S.-S. Zhang, Z. M. Raines, and A. V. Chubukov, Applicability of eliashberg theory for systems with electron-phonon and electron-electron interaction: A comparative analysis, Phys. Rev. B **109**, 245132 (2024).

[38] A. V. Chubukov, D. Pines, and J. Schmalian, A spin fluctuation model for d-wave superconductivity, in *The Physics of Superconductors: Vol. I. Conventional and High-T_c Superconductors* (Springer, Berlin, Heidelberg, 2003), pp. 495–590.

[39] A. V. Chubukov, A. Abanov, Y. Wang, and Y.-M. Wu, The interplay between superconductivity and non-fermi liquid at a quantum-critical point in a metal, Ann. Phys. **417**, 168142 (2020).

[40] A. Abanov and A. V. Chubukov, Interplay between superconductivity and non-fermi liquid at a quantum critical point in a metal. i. the γ model and its phase diagram at $T = 0$: The case $0 < \gamma < 1$, Phys. Rev. B **102**, 024524 (2020).

[41] Wikipedia, Airy function—Wikipedia, the free encyclopedia, http://en.wikipedia.org/w/index.php?title=Airy%20function&oldid=1274965224 (2025) [Online; accessed 07-March-2025].

[42] R. Shankar, Renormalization-group approach to interacting fermions, Rev. Mod. Phys. **66**, 129 (1994).

[43] J. Polchinski, Effective field theory and the Fermi surface, arXiv:hep-th/9210046.

[44] R. Nandkishore, L. Levitov, and A. Chubukov, Chiral superconductivity from repulsive interactions in doped graphene, Nat. Phys. **8**, 158 (2012).

[45] A. V. Chubukov and J. Schmalian, Superconductivity due to massless boson exchange in the strong-coupling limit, Phys. Rev. B **72**, 174520 (2005); Pairing glue in cuprate superconductors from the self-energy revealed via machine learning, **101**, 180510(R) (2020).

[46] A. Abanov, S.-S. Zhang, and A. V. Chubukov, Non-BCS behavior of the pairing susceptibility near the onset of superconductivity in a quantum-critical metal, Phys. Rev. B **111**, 075157 (2025).